Effect of flap angle on transom stern flow of a High speed displacement Surface combatant

Y. Hemanth Kumar[*] and R. Vijayakumar[**]

Department of Ocean Engineering, Indian Institute of Technology, Madras, India

Abstract. Hydrodynamic Drag of Surface combatants pose significant challenges with regard to fuel efficiency and exhaust emissions. Stern flaps have been used widely as an energy saving device, particularly by the US Navy (Hemanth *et al.* 2018a, Hemanth Kumar and Vijayakumar 2018b). In the present investigation the effect of flap turning angle on drag reduction is numerically and experimentally studied for a high-speed displacement surface combatant fitted with a stern flap in the Froude number range of 0.17-0.48. Parametric investigations are undertaken for constant chord length & span and varying turning angles of 5° 10º & 15°. Experimental resistance values in towing tank tests were validated with CFD. Investigations revealed that pressure increased as the flow velocity decreased with an increase in flap turning angle which was due to the centrifugal action of the flow caused by the induced concave curvature under the flap. There was no significant change in stern wave height but there was a gradual increase in the stern wave steepness with flap angle. Effective length of the vessel increased by lengthening of transom hollow. In low Froude number regime, flow was not influenced by flap curvature effects and pressure recovery was marginal. In the intermediate and high Froude number regimes pressure recovery increased with the flap turning angle and flow velocity.

Keywords: ship hydrodynamics; stern flow; transom stern; stern flap

1. Introduction

Stern flaps (flaps affixed at the transom stern end. Fig.1) are used on high speed displacement vessels to decelerate the flow along the stern underside and convert the dynamic flow pressure to static wall pressure on the hull, thereby increasing the pressure under the transom stern. Increase in the stern underside pressure creates a pressure force vector which includes a thrust component on the hull which is known to reduce the resistance. In addition to this, the stern flap has also been known to attenuate the stern wave contributing to the resistance reduction. Depending on the hull form and design speed range, stern flaps have been designed in different configurations. Flow characteristics near the stern end are strongly dependent on the flow velocity and the curvature induced by the flap turning angle. Optimum stern flap geometry is based on model tests and CFD analysis of various flap configurations. Several research groups (Karafiath *et al.* 1999, Cave 1993, Karafiath *et al.* 2001, Thornhill *et al.* 2008, Maki *et al.* 2016, John *et al.* 2011) conducted

∗Corresponding author, Ph.D. Student, E-mail: hemanthnavy@gmail.com
∗∗ Assistant Professor, E-mail: vijay2028@iitm.ac.in

systematic model tests and parametric investigations to determine optimum flap geometry. While research has been conducted on the effect of stern flaps in resistance reduction, targeted study on influence of flap geometrical parameters on the physics of flow modification in the transom stern region have been limited. Important aspects of streamline curvature effects causing radial pressure gradients and its relationship with reduction in resistance have not been studied. Study of local changes in the stern flow with a consequent resistance reduction have also been limited. This work aims to analyze flow behavior under a stern Flap with the help of CFD using the STAR CCM+ software for study of flow and consequent resistance measurements using model test experiments in towing tank. An attempt has been made to study the effect of flap turning angle on various flow parameters viz. static pressure rise at the inflection plane caused by the flap, flow velocity, and development of stern flow with regard to attenuation of stern wave profile are considered in this analysis.

2. Experimental setup

Review of several studies w.r.t stern flaps fitted on high speed displacement vessels was undertaken to establish the dimensions of model hull. Main particulars are indicated at Table 1.
Literature survey indicated that stern flaps are usually semi-elliptically shaped with faired corners. From the survey of typical stern flap dimensions, flap configurations with a constant chord length of 1% L_{BP}, constant span of 60% transom width and three flap turning angles 5° 10° & 15° were selected to undertake the studies. Model draft of 0.123 m in even keel condition, was selected as a representative loading condition of the hull model. Based on the selected dimensions of the model and limiting the blockage to be less than 10%, a scaled model of 1:35 was considered to be appropriate. Accordingly, the analysis of transom flow-stern flap interaction was undertaken on FRP model of a generic high-speed displacement surface combatant fitted with typical stern flaps with constant chord length & span and varying flap angles as shown in Fig. 1.
Experimental studies were undertaken to study the resistance of a scaled model in the towing tank facility at IIT Madras which has the dimensions of 85 m x 3.2 m x 2.5 m with a maximum carriage speed of 5 m/s, to study the effect of stern flap fitted at the transom end with varying turning angles. The experimental setup is schematically shown in Fig. 2.

Table 1 Details of Hull

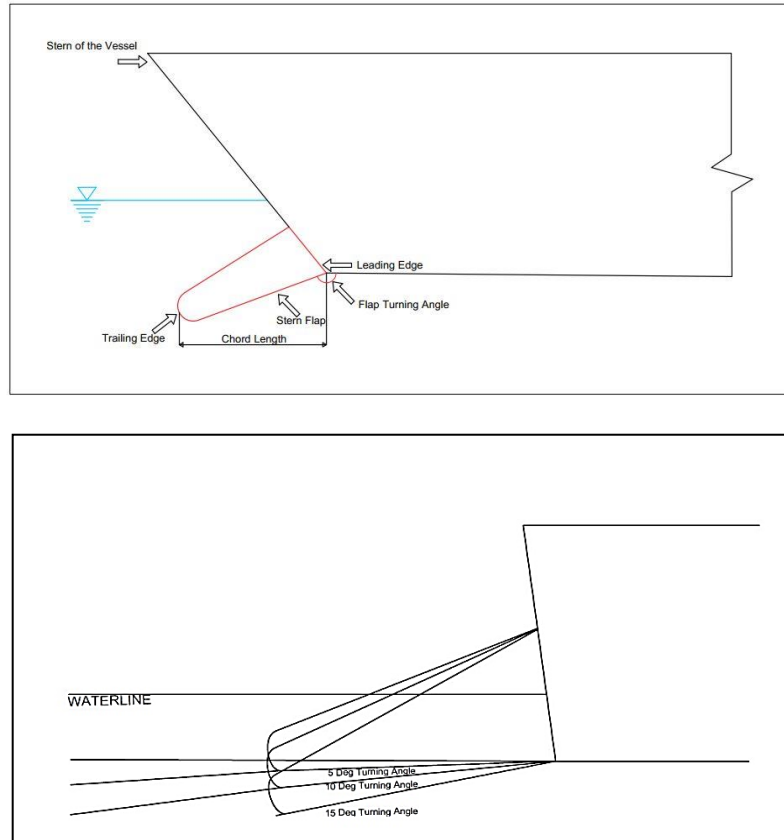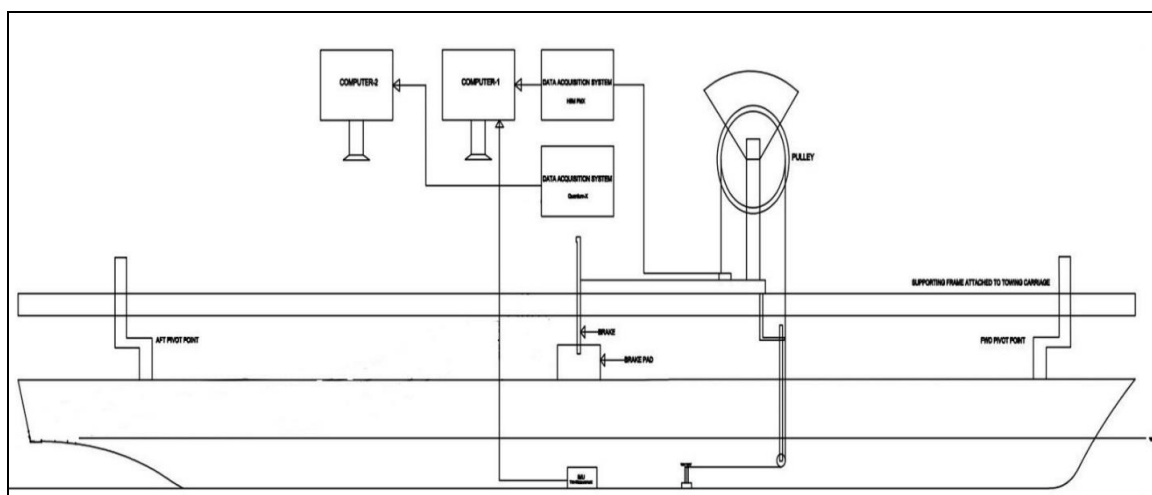| Parameters	Model
L_{OA}	4.11 m
L_{BP}	3.87 m
Breadth extreme, B	0.485 m
Transom width, B_T	0.362 m
Draft, T	0.123 m
Displacement	110.74 kg
Froude no range	0.17-0.48

Fig. 1 Configuration of Stern Flaps

Fig. 2 Schematic of experimental setup in towing tank

A load cell of 50kg was mounted on the support frame of the resistance testing module to measure the drag values. The hull model was fixed to the towing carriage by using two pivot levers and supported by a brake pad. Motion Reference Unit (MRU) was mounted on the model to measure the dynamic trim.

3. CFD modelling and validation

In order to study the modification of stern flow by the flap, CFD study was undertaken. For the study a bare hull model (scale of 1:35) was first generated in CAD software (Rhino) which was then modeled in commercial CFD software Star CCM+. In this package, the differential form of Navier-Stoke equations combined with Reynolds averaged form of N-S equations are solved for solution to the governing equations. For the purpose of closure of Reynolds stress terms, k– ε turbulence model has been used. Volume of Fluid (VOF) method has been used to capture the wave free surface effects. Dynamic Fluid Body Interaction (DFBI) method has been used to couple fluid-body motions. The basic numerical validation included comparison of the bare hull drag and hull with three flap turning angles, which is obtained from the pressure integration from the RANSE solver and comparing with experimental results obtained in the towing tank tests.

3.1 Setup of computational domain

Modelling of the Computational domain was undertaken as per ITTC Guidelines (ITTC - Recommended Procedures and Guidelines 7.5-03-02-03, 2011). For the purpose of the present investigations, a rectangular domain is utilized. The inlet exterior boundary is placed at 1L distance from the hull, whereas the outlet boundary is located at 4L distance from the hull. Top and bottom boundaries are at 1L and 2L distances, respectively from the hull. Distance between side boundary and symmetry plane was taken as 2L. Since the hull model is symmetric about the centerline and in order to reduce the computational time, half hull model was used for the numerical simulations. Details of the domain boundaries are shown in Fig. 3 below.
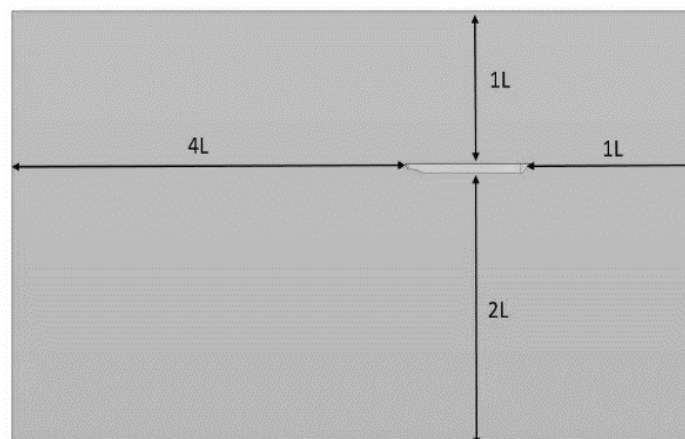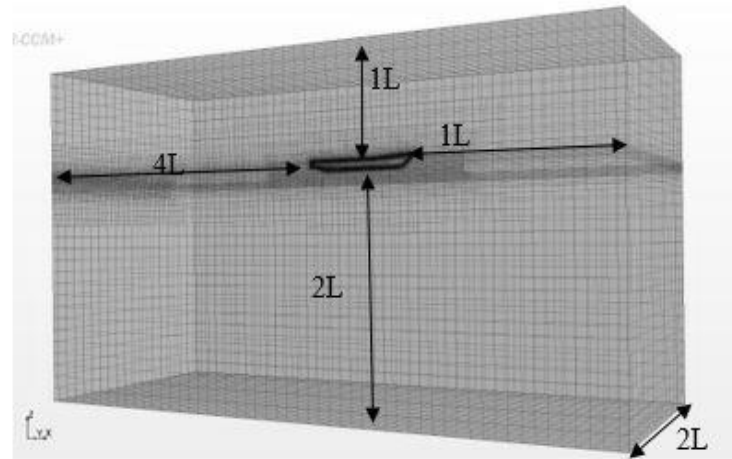

Continued-

Fig. 3 Set-up of Computational Domain

3.2 Generation of computational grid

In order to improve the quality of the solution, a combination of structured and unstructured grids have been used. The Finite volume computational solver for the domain was discretized
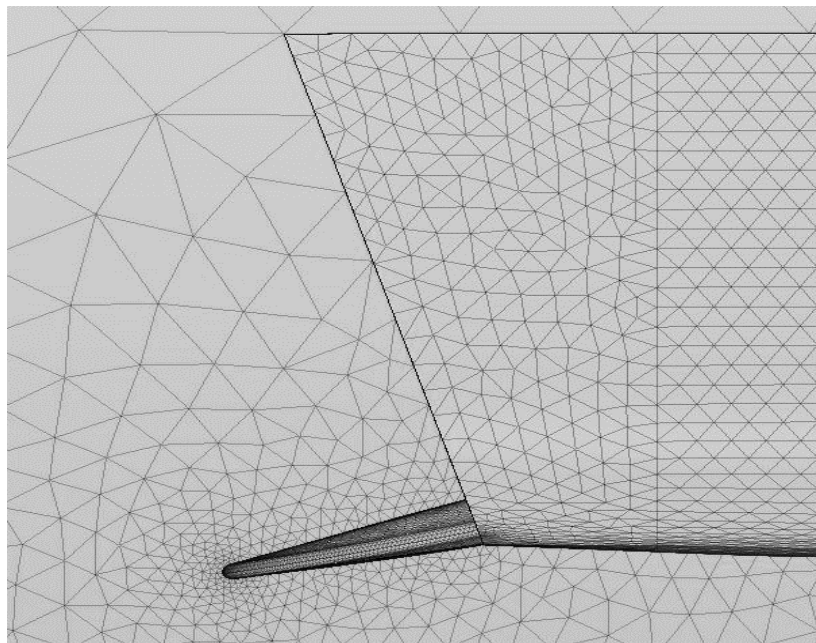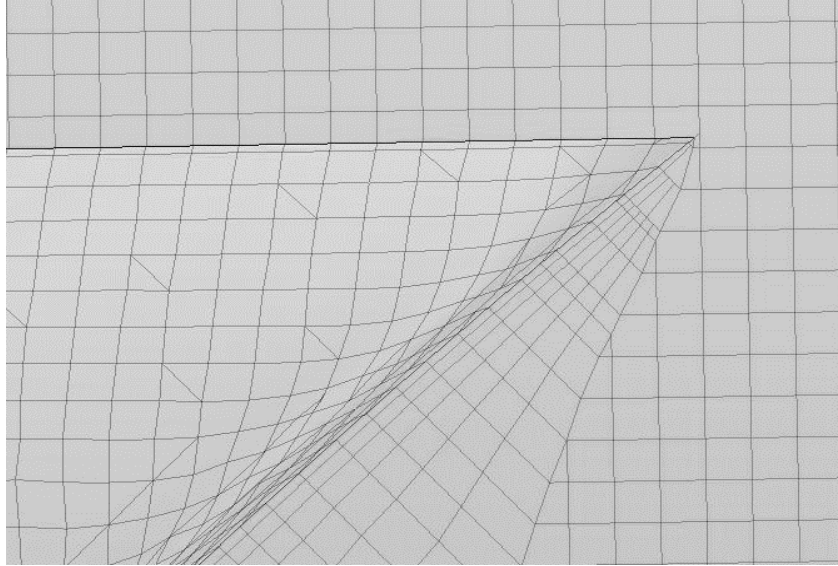

Fig. 4 Surface Mesh of the hull form

Fig. 5 Prism Layer and Volume mesh in the vicinity of the hull

using hexahedral cells. Trimmer was utilized to trim these hexahedral cells to form polyhedral cells in the vicinity of the hull surfaces to accurately capture the surface curvatures. In the areas around the hull, near field transom stern region and Kelvin wave region, volume grids were generated in order to capture the free-surface effects and flow pattern. In order to capture high flow gradients inside the boundary layer close to the ship hull, prism layer meshing has been used. Surface mesh generated for the hull form is presented in Fig. 4, Prism layer mesh and fine volume mesh around the hull are shown in Fig. 5.

3.3 Grid independence study

Grid independence study was undertaken to minimize the discretization errors due to the discretization of the computational domain in to control volumes. Simulations were started initially with coarse meshing and thereafter was progressively refined to finer mesh by dividing the base size by a factor of $\sqrt{2}$. In this study, total resistance of the model hull was used as the criteria for monitoring the Grid independency.

Table 2 Grid independence Study

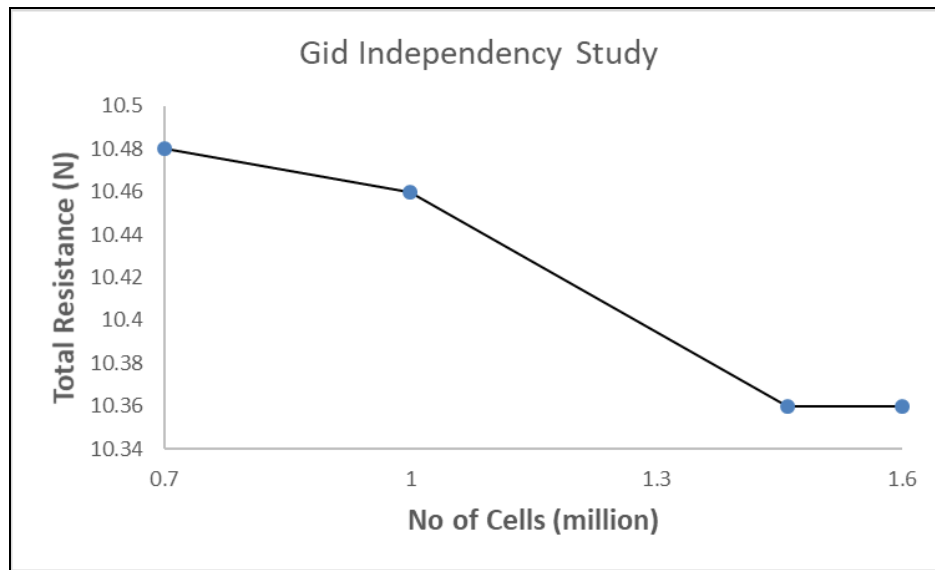| No of cells (millions)	Model Resistance (N)
0.7	10.48
1	10.46
1.46	**10.36**
1.8	10.36

Fig. 6 Resistance Values-Grid independence Study

Using each mesh formation, the simulation was undertaken for hull model fitted with flap of Chord length 1% model length, 60% model transom width and turning angle of 5° corresponding to the Froude number of 0.25. The total resistance value for each case is tabulated in Table 2 and plotted in Fig. 6. Based on the Grid independence study, the grid independent solution was arrived at a grid configuration with 1.46 million cells. This configuration was used for further study.

3.4 Boundary conditions

In order to solve the governing equations, both boundary conditions and initial conditions are required to be defined. Table 3 specifies the details of the boundary conditions-imposed.

3.5 Validation

The CFD model used in this study was validated with the experimental resistance results obtained in towing tank tests on without flap and with flap conditions (5°, 10° & 15°). Resistance trends obtained computationally for all conditions matched fairly well with experimental data (Figs. 7-10).

Table 3 Boundary Conditions

Surface	Boundary Condition
Model Hull	Wall
Domain Inlet (ahead of vessel), Side, Top and Bottom	Velocity inlet
Domain Outlet – Behind the vessel	Pressure outlet
Domain – Centreline Plane	Symmetry Plane

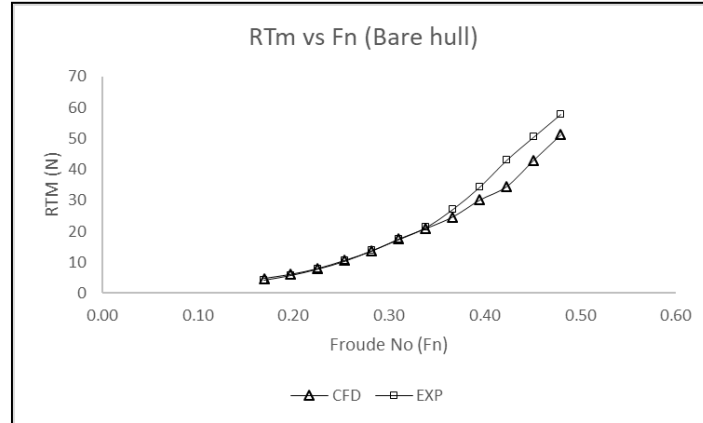*Y. Hemanth Kumar and R. Vijayakumar*

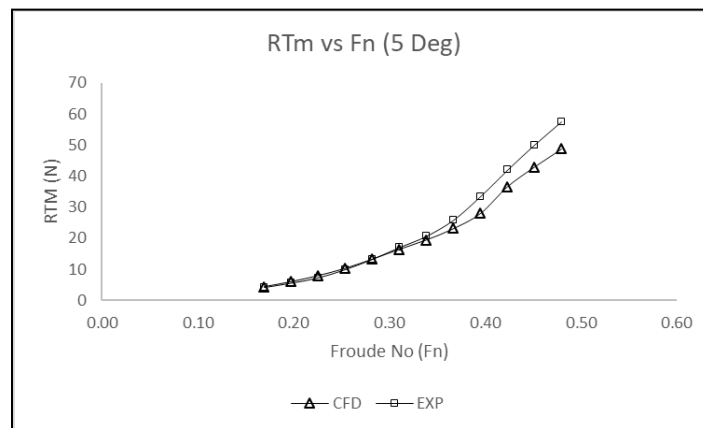Fig. 7 Experimental vs Numerical Resistance values (Bare hull Condition)

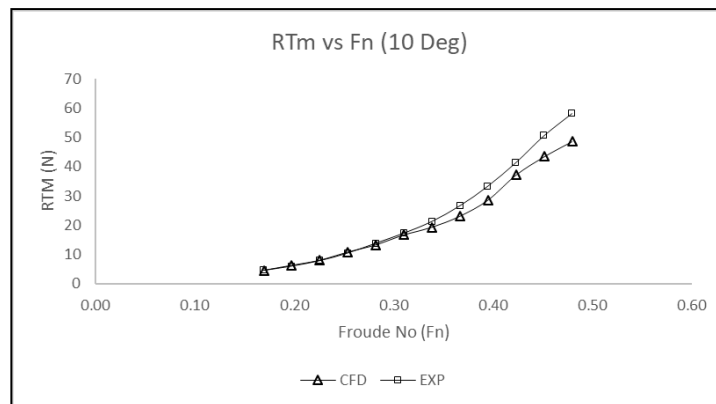Fig. 8 Experimental vs Numerical Resistance values (5º Flap)

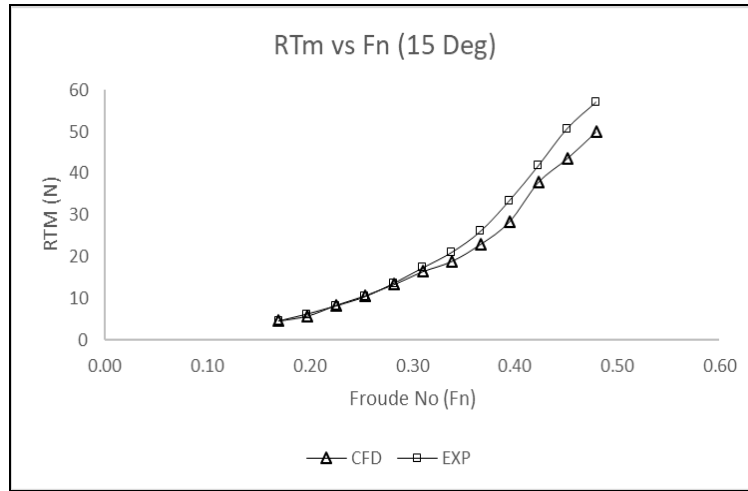Fig. 9 Experimental vs Numerical Resistance values (10º Flap)

Fig. 10 Experimental vs Numerical Resistance Values (15º Flap)

The comparison between CFD & experiment data in all conditions shows good agreement at lower Froude numbers. Deviations in intermediate and higher Froude number range is of the order of 10% which is reasonably accurate and can be used for carrying out further investigations.

4. Results & discussion

Results of Parametric investigations undertaken in CFD by varying flap turning angle (θ) at the highest Froude number of 0.48 are discussed since the variation in performance parameters are manifest distinctly.

4.1 Pressure distribution

Performance evaluation of a stern flap fitted on ship transom end is analyzed in terms of conversion of dynamic flow pressure to static wall pressure due to curvature induced by the flap turning angle. This is represented as coefficient of pressure (Cp) (Lars Larsson 2010)

$$Cp = \frac{(Ps + \rho gh)}{(0.5\rho v^2)}$$

(Lars Larsson 2010) discussed the mechanism by which pressure gradients are created on the hull due to curvature effects. As the fluid flows around the ship, pressure gradients are developed across the streamlines with a corresponding centripetal force directed towards the center of curvature due to the curvature of hull. The relation is given by the Euler's equation

$$\frac{\partial P}{\partial R} = \frac{\rho V^2}{R}$$

This pattern of development of pressure gradients in using the streamline curvature argument is used to explain the mechanism of pressure recovery due to stern flap. The flow approaching the stern from the forward part of the vessel flows along the stern contour where the local radii of curvature (R) continues to increase. However, the local radius of curvature reduces drastically due to the concave curvature induced by the flap turning angle near the transom edge where the flap meets the hull. As the flow approaches the transom edge, it starts feeling the presence of the flap induced curvature and as a result, there is a rise in the pressure as compared to the no flap condition. (Lars Larsson 2010) explained that at locations were the flow moves over concave curvatures the pressure increase occurs on the hull side to balance the centrifugal acceleration of fluid particles. Increase in the pressure under the stern generates the pressure force vector, which includes a forward thrust component which reduces the resistance. Parametric study in CFD for different flap turning angles 5°, 10° and 15° was undertaken. It was observed that with an increase in the turning angle the concave radius of curvature decreased in the underside of the hull thereby increasing the pressure. Coefficient of pressure (Cp) was observed to be maximum at a flap with a turning angle of 15°. This behavior is clearly illustrated in the C_P distribution presented in the Figs. 11 and 12.
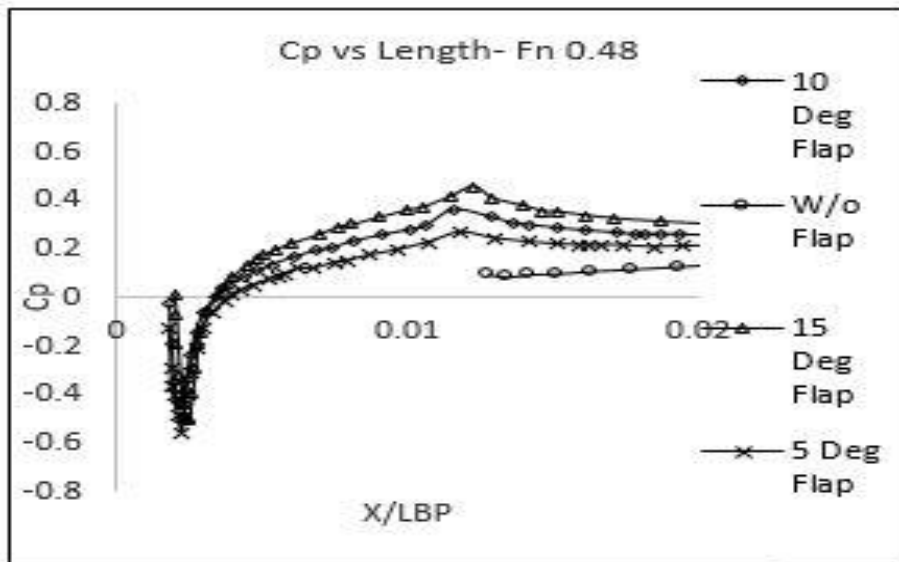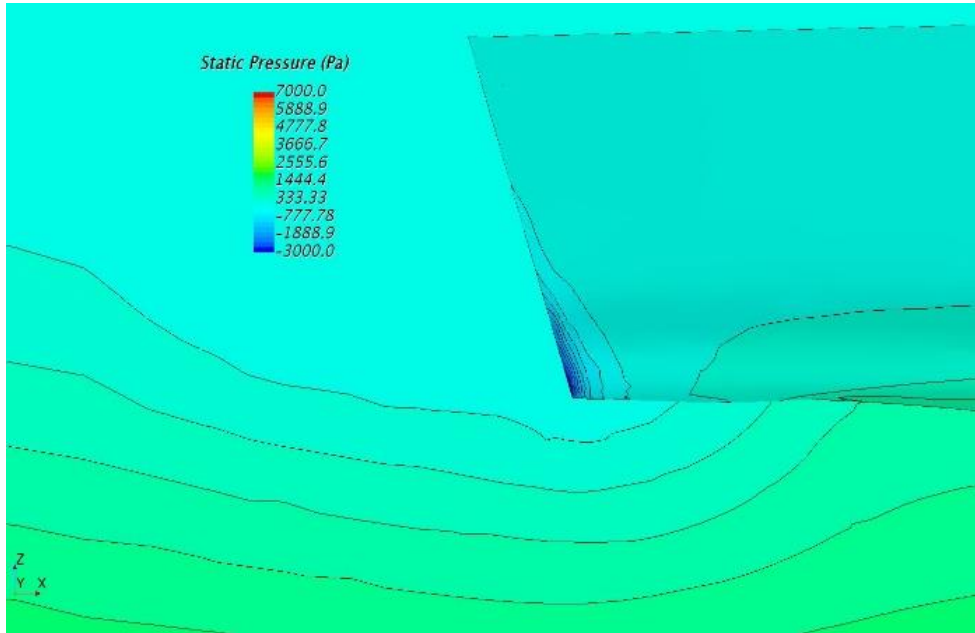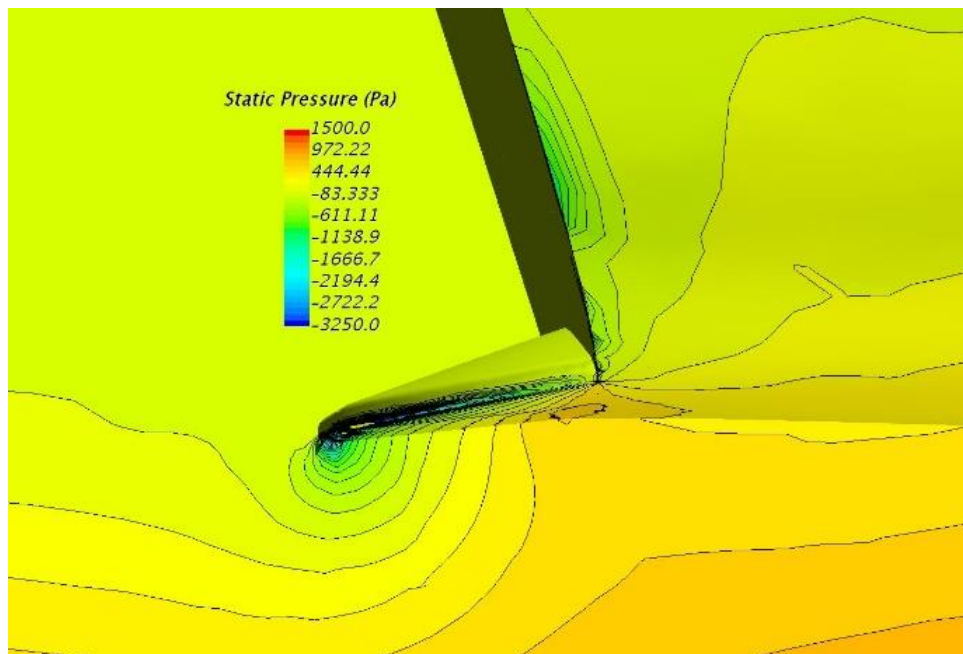

Fig. 11 Coeff of Pressure (Cp) plotted along Model length at Stern region

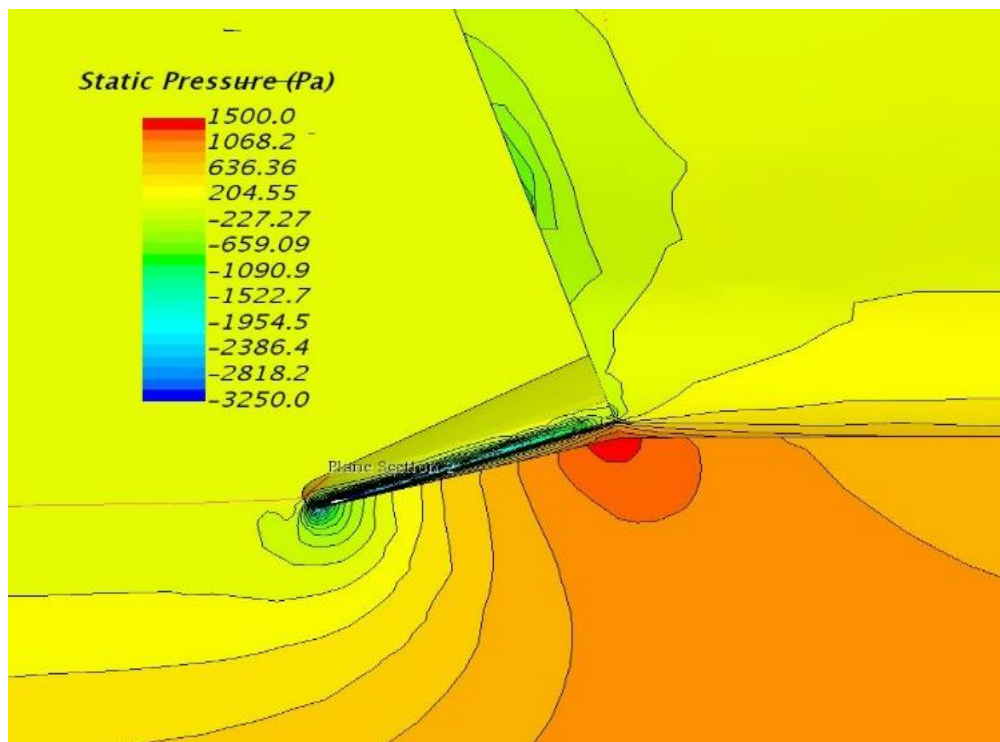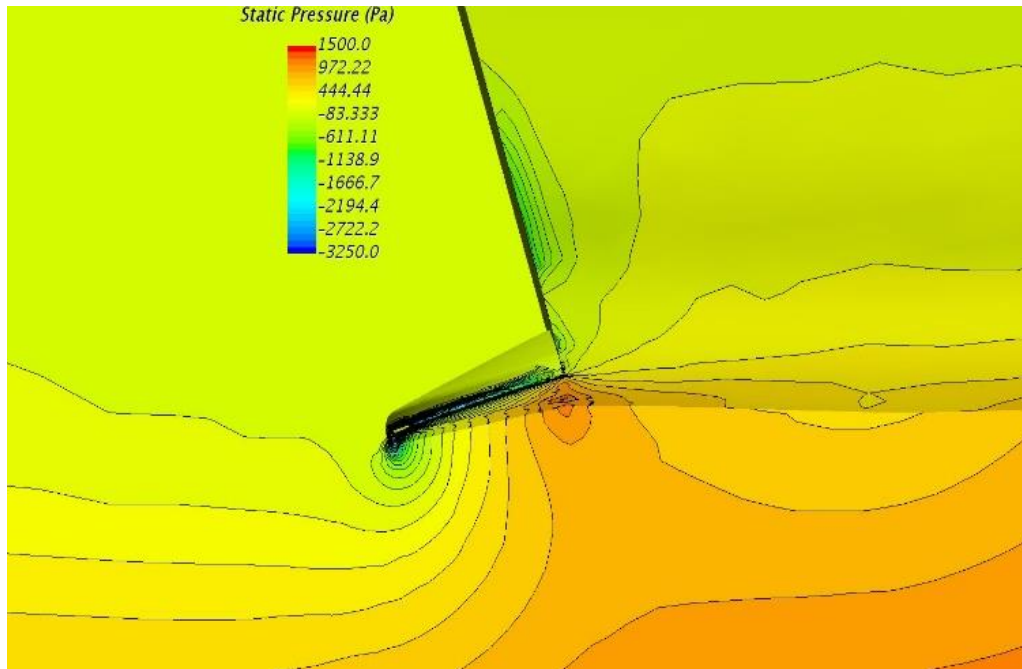**Bare Hull**

5 DEG

10 DEG

Continued-

15 DEG

Fig. 12 Contour Plots of Coeff of Pressure (Cp) plotted along Model length at Stern region

4.2 Velocity distribution

Longitudinal variation of the streamline velocity in the symmetry plane of ship hull with & without flap fitted with 5°, 10° and 15° turning angle is presented in Figs. 13 and 14.

From the Euler's expression it follows that for a given pressure gradient across the streamlines the smaller the radius of curvature that the fluid particle follows, smaller is its velocity along the streamlines. The stern flap added at the transom edge drastically reduces local radius of curvature which correspondingly decreases the local flow velocity. As the flow moves from this region of high curvature on to the chord length of the flap which has a relatively higher local radius of curvature this region experiences flow with high velocities. Analogous to the case of hull pressures, the maximum reduction in flow velocity at the transom edge was achieved by the 15° flap which induced maximum local concave curvature as compared to the 5° and 10° flap. This behavior is clearly observed in the Velocity distribution presented in the Fig. 13. Longitudinal velocity distribution along the stern contour can also be analyzed by studying the Iso-velocity flow contours (Fig. 14). In these figures, red and blue color indicate high speed and low speed flow respectively. It can be seen that the flow development is symmetrical in nature about the keel centerline throughout the length of the ship. In the stern region fitted with stern flap, an inflection point, which does not appear in the original hull form appears and creates a curved concave surface at the transom edge. The flow development along the underside of the stern contour is characterized by the momentum transfer towards the concave underside of the hull and also by the radial pressure gradient, due to curvature effects. In the without flap condition, from contour plots it can be seen that high velocity flow occupies the stern contour area and continues to increase leading up to the exit at transom edge.
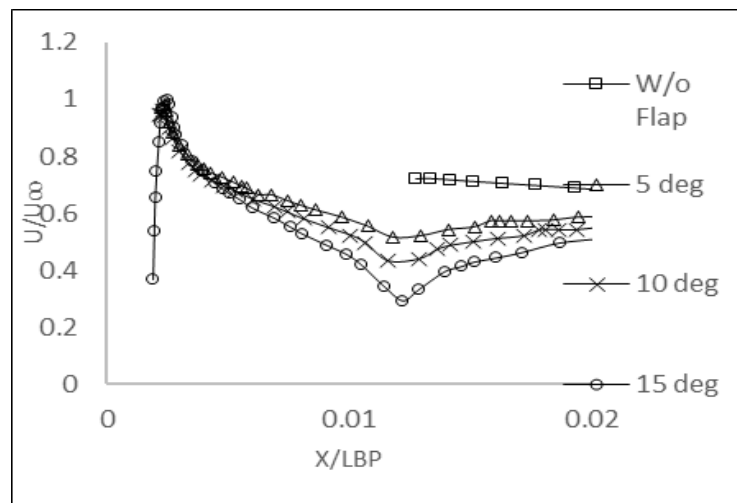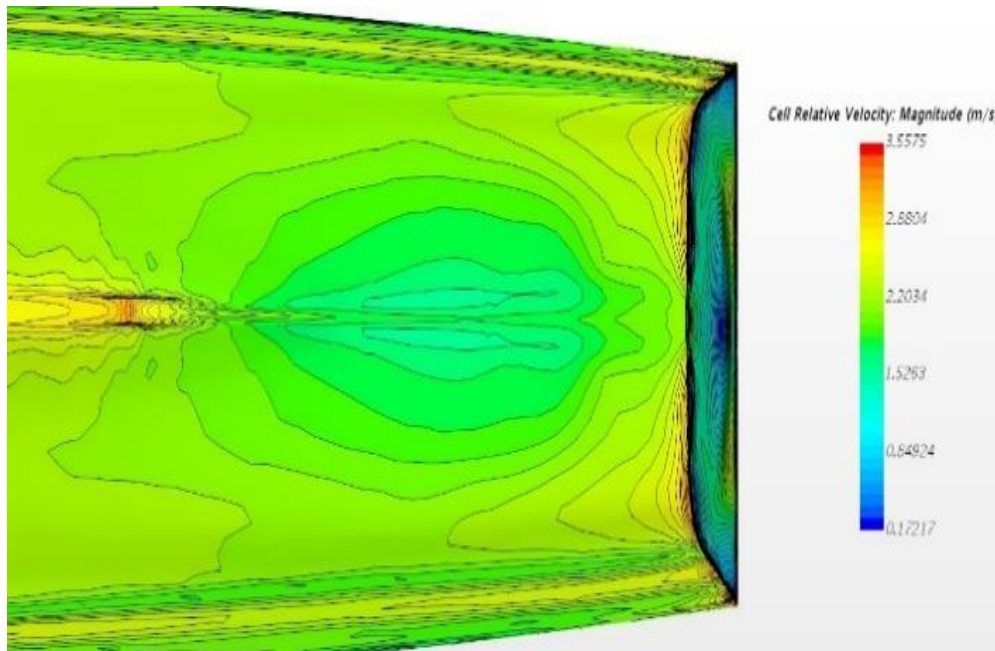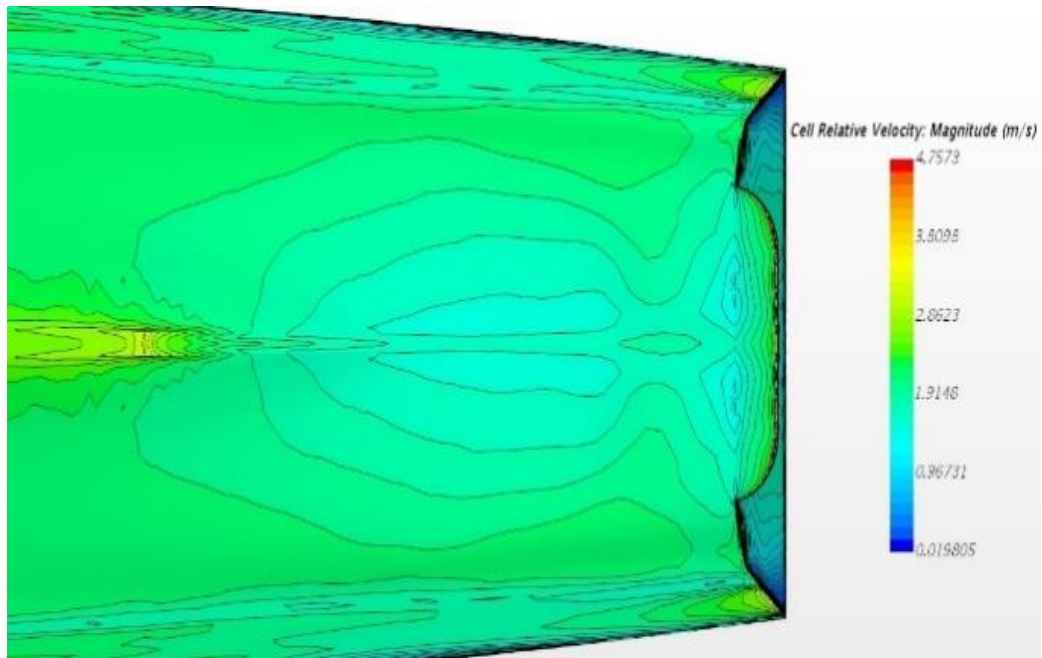

Fig. 13 Coeff of Velocity plotted along Model length at Stern region
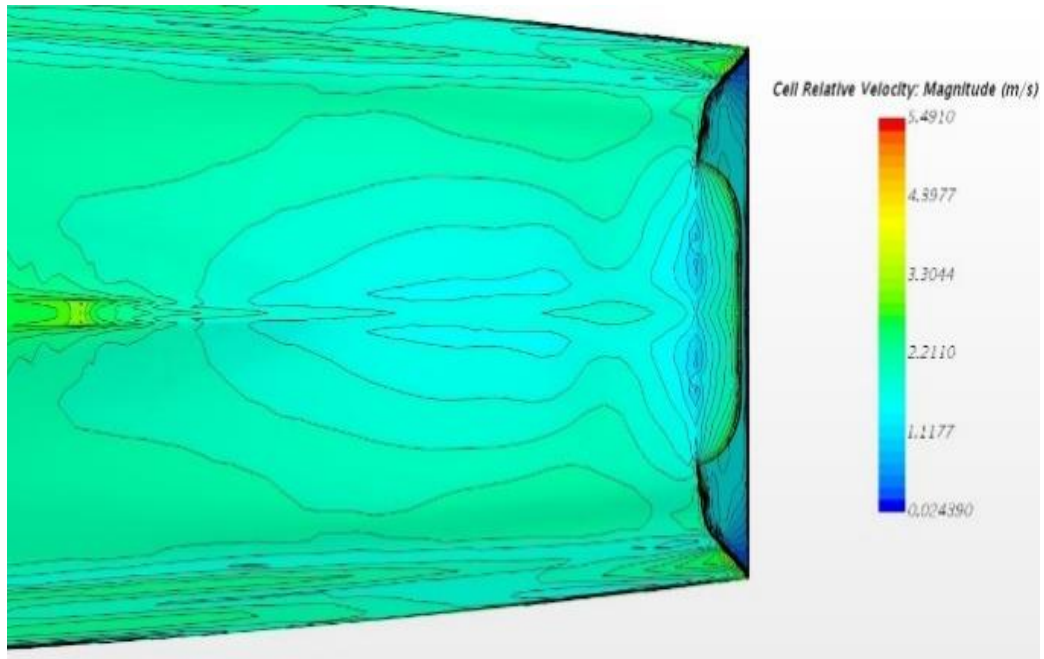
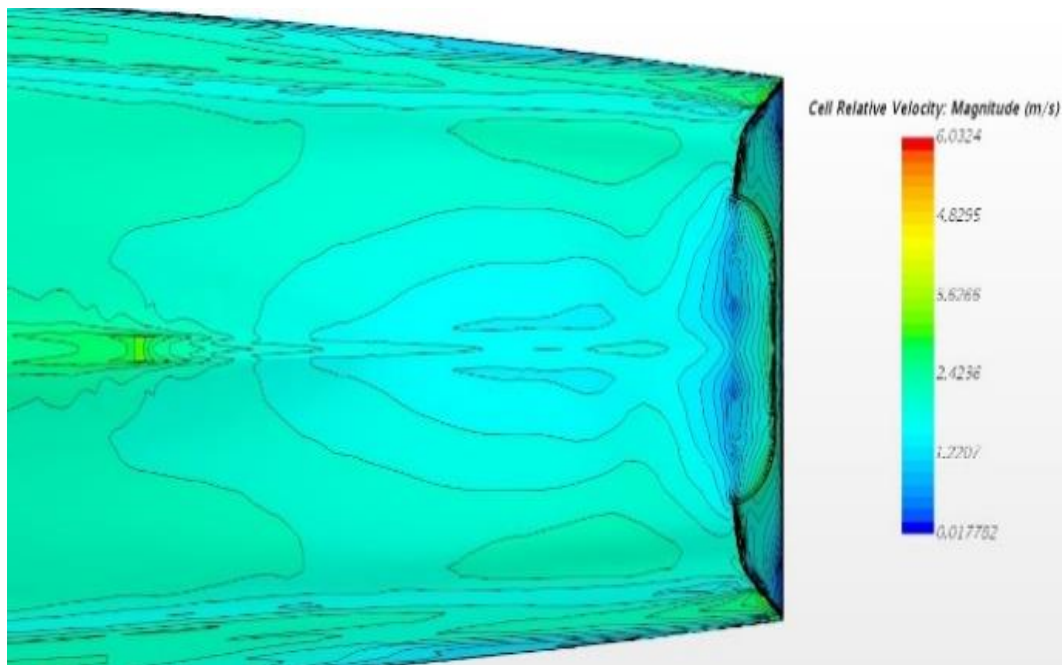**5 DEG**

10 DEG

Contineud-

15 DEG

Fig. 14 Contours of Coeff of Velocity plotted along Model length at Stern region

However, in the model hull with stern flap the flow velocity decreases as it approaches the Stern flap and it is considered that much of this decrease is due to the flow turning caused by the stern flap. Because of the curvature, rapid movement of flow occurs from the forward portion of the flap-transom edge to the concave wall. It appears that the effect of flap causing decrease in the flow velocity, holds not only for the concave region close to the flap but is felt all along the stern contour away from the flap. It is also seen that with the increase in the flap turning angle, shape of the flow pattern along the stern contour does not change drastically but we observe low velocity flow accumulation at the concave wall created by flap-transom intersection.

4.3 Stern flow development

After the analysis of Pressure-Velocity variations along the fore-aft stern contour, investigations proceeded by studying the flow characteristics in the near-stern region, specifically the development of stern waves and transom hollow, which were considered to be the principal contributors impacting resistance.

4.3.1 Wave height

Firstly with regard to development of stern waves, several studies (Tadao Yamano et al. 2003) have been undertaken to study the effect of stern profile on resistance. They reported that flow leaving the transom edge of the vessel will have an upward component of the flow velocity which would carry the unused flow energy astern. This upward oriented flow near the stern-end of the vessel plays an important role in the generation of stern waves and the presence of stern end device (such as a stern flap) can attenuate/ weaken the stern waves by reducing the slope of the wave profile through suppression of the upward oriented flow. This suppression in-turn causes reduction in the resistance. Wave profile patterns were analyzed for the hull model in without flap and with flaps condition. Computational rooster tail and Wave Profiles obtained along the symmetry plane behind the transom stern are shown in the Fig. 15.

It can be seen that the crest of the stern wave in without flap condition is close to the stern end plane. For the model with stern flap whose flap end is lower than the still water level, flow under the transom bottom cannot rise immediately due to blocking effect of the stern flap. It was observed that the crest of the Stern wave moved further downstream relative to the without flap (w/o) condition. As the flap turning angle increased it was observed that there was a gradual shift in the crest of the wave downstream. While there was no appreciable difference in the wave heights between bare hull and 5º &10º flap condition, the stern wave height increased substantially for 15º flap angle which could be the limiting criteria for determining the optimum flap turning angle and an attempt will be made to explain the limiting condition in the subsequent paragraph. From the observations, it was concluded that as the flap angle increased from 5º to 15º, wave height increased.

It may be recalled from the discussions at Section 4.1, that the increase in the flap turning angle from 5º to 15º increased the pressure under the transom hull measured at the centerline. Now that the development of stern wave pattern has been analyzed, we shall now try to explain the influence of flap induced pressure underneath the transom caused by the turning angle on development of transom wave heights. In without flap condition, as the flow from beneath the transom leaves it experiences sudden change in pressure (i.e., from high pressure to atmospheric pressure) which leads to an increase in the flow velocity and thereby the wave height.
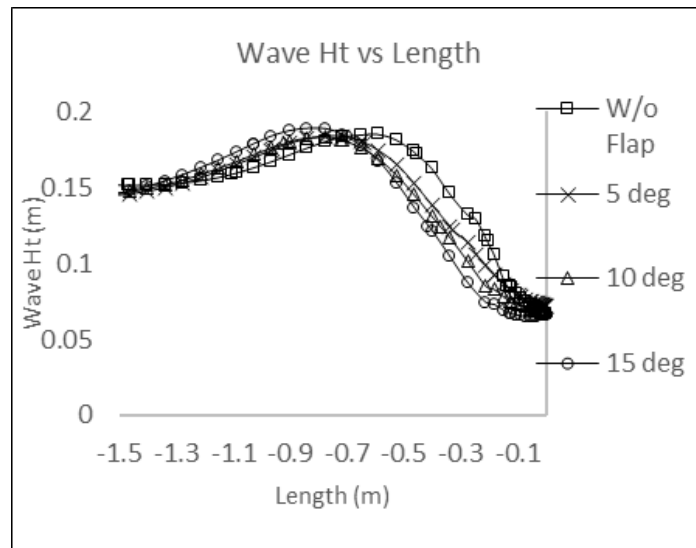
Fig. 15 Stern Wave profiles in with and without flap condition

However, in case of the present model fitted with a flap, we have seen from Fig. 4 that a sharp increase in the pressure under the transom edge is caused due to the flap turning angle. When the flow moves from underneath the transom it experiences remarkable pressure difference relative to w/o flap condition.

As the flap turning angle was increased from 5º to 10º and to 15º, the pressure continued to increase under the transom. As the flow left the stern flap trailing edge, it experienced an abrupt change in pressure which caused sudden increase in flow velocity leading to the formation of a steep wave profile behind the transom which explains why the wave profile of a 15º flap was steeper than other flap angles. Based on the observations so far, we can reasonably anticipate that in order to reduce the transom stern wave height (which is a measure of wave resistance), the pressure variation underneath the flap will have to be altered, mindful of the fact that certain pressure increase is required for generation of the lift vector to counter resistance. Since, flap turning angle plays a pre-dominant role in inducing pressure increase, one of the important limiting criteria for determining the optimum flap turning angle is wave height reduction, while there is adequate lift in the direction of motion.

4.3.2 Characteristics of hollow

After analyzing the stern wave heights, the development of transom hollow, which is typical to transom sterns was analyzed. (Doctors *et al.* 2007, Doctors 2006) reported that in dry transom regime a trough shaped depression or a hollow is formed behind the Stern due to hydrodynamic suction created by the flow behind the transom. They showed that the transom hollow could be considered to virtually extend the effective hull length with no increase in the wetted surface area and friction drag. For the present hull fitted with Stern flap, it has been observed both in numerical analysis and experiments that as the ship's transom moved from rest through various speed regimes the water dragged behind the transom in the lower Froude numbers i.e., from 0.17 to 0.28. In this regime it was seen that the eddies created due to flow separation at the bottom and sides of the transom continuously filled the region behind the transom. However, as the Froude no

approached 0.31, the water appeared to separate cleanly from the transom bottom. Eddy formations were diminished and the water appeared like a sheet leaving from the transom bottom creating a hollow, which has been observed both during the model experiments and in CFD. At this instant when the water from the transom bottom cleanly separated, the transom of the model was completely dry. In order to analyze the development of hollow as a function of flap turning angle, numerical analysis was resorted to. As the turning angle of the flap was gradually increased from 5º, 10º and 15º the length of the hollow that has been created behind the stern end, got longer up to a point were the Rooster tail is formed. The variation of the length of the hollow cavity as a function of flap angle is shown in Fig. 16. The results presented below correspond to a Froude number 0.48. The same trend has been observed for all Froude numbers above 0.31.

From the analysis, it was observed that an increase in the flap turning angle increased the length of the hollow there by increasing the effective length of the vessel. As the effective vessel length increased, the effective length Froude number of the vessel decreased thereby having the potential to positively contribute in the resistance reduction, provided there is an adequate pressure recovery under the transom coupled with a decrease in the stern wave heights.
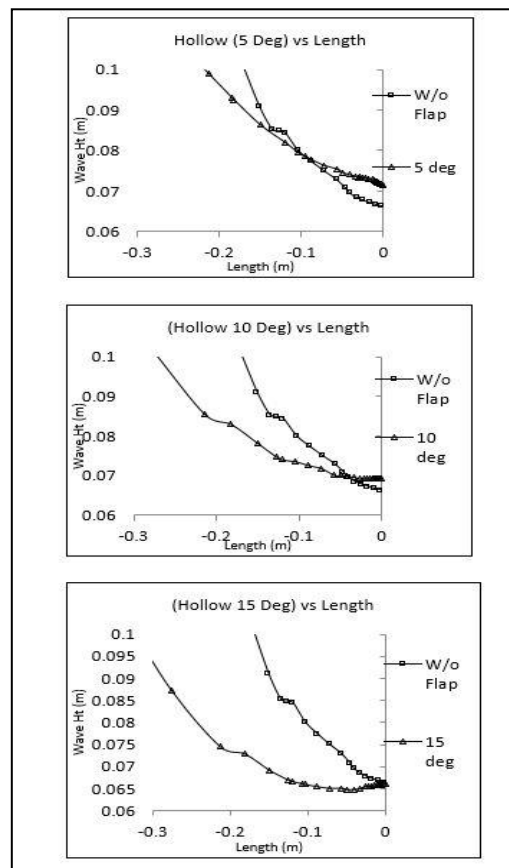

Fig. 16 Variation of Hollow length with Varying Flap angle

5. Effect on resistance

In the previous sections, analysis of various results revealed that pressure recovery under then flap, reduction in stern wave heights and creation of transom hollow together contribute to the decrease in the resistance. It was also seen that the onset of clean flow separation from the transom edge/ flap edge (i.e., when the transom becomes dry at Fn = 0.31) is a prerequisite for the formation of the Transom hollow. In order to summarize the analysis undertaken and to understand the effect of flap on the resistance reduction, analysis is presented into two regimes i.e., in the wetted transom regime where there is eddy formation and dragging of water behind stern and dry transom regime where there is a clean flow separation and transom hollow formation. Before examining the resistance, the effect of increase in the pressure on the hull underside due to flap on causing running trim was examined numerically in order to ascertain the extent to which trim changes to be able influence the resistance. In the below plot (Fig. 17) trim is indicated in degrees and negative angle indicates trim by Stern.

Due to the addition of stern flap it was observed that there was no significant change in trim as compared to the w/o flap condition. Only a marginal reduction was observed in the bow up trim. This was because, unlike in planning hulls where flap causes significant changes in trim, in case of displacement hull the hydrodynamic forces due to flaps acting upon the hull are inadequate to create trim angles of more than several degrees and the changes in trim experienced by the hull do not impact resistance significantly. As a consequence, there was no significant change in the trim or changing utmost by marginal percentage. Therefore the change in trim due to flap & hence resistance is negligible. Once it was established that the trim was negligible, effect of flap on total resistance was investigated. Total resistance estimated numerically at each Froude number in with & without flap condition is indicated in Fig. 18 below

5.1 Low Froude number regime (0.17-0.25) – Wet Transom

This regime is characterized by low velocity flows. At these Froude numbers, the flow was not greatly influenced by curvature effects induced by the flap.
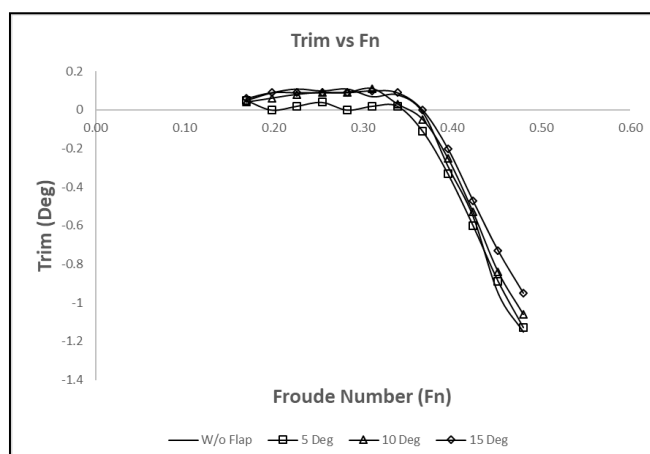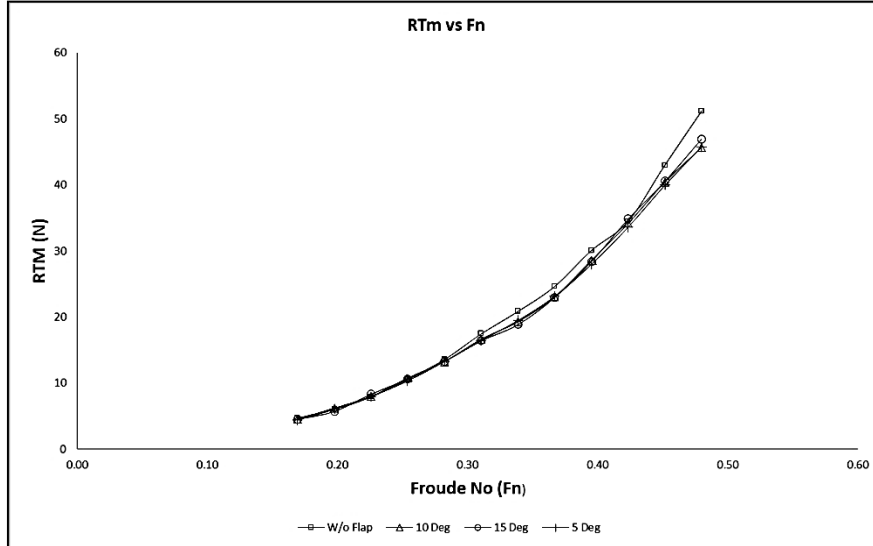

Fig. 17 Trim vs Froude number

Fig. 18 Total Resistance vs Froude Number

At these speeds, the transom was immersed and pressure on the over side of the stern flap was of the order of magnitude comparable to the pressure on the underside of the flap since the difference in heights of the over & undersides is very small. Although the camber induced by stern flap causes pressure recovery on the hull, the magnitude of such a pressure recovery is insignificant due to the low freestream velocities, to yield any reasonably large forward thrust component to cause a decrease in the resistance. As has already been discussed at Para 4.3.2, at these low Froude numbers the flow did not separate tangentially from stern bottom and it appeared that the transom stern dragged the water, in a narrow zone behind the transom. Further, as can be seen in the Fig. 19 below, the depth of transom immersion estimated numerically from the static waterline is of the order of approx. 5% of the transom depth and this value falls to zero i.e., the transom fully ventilates at Froude number 0.31. Therefore, in this regime the contribution from hydrostatic force for assisting the forward motion is negligible, since transom is mostly dry. Low pressure recovery due to flap coupled with viscous resistance, minimum hydrostatic forward component on the transom and non-existence of transom hollow results in no reduction in resistance irrespective of any flap turning angle as evident from the resistance curves for with and without flap condition shown in Fig. 18.

5.2 Intermediate Froude number regime (0.28-0.37)

The transom becomes dry after the Froude number 0.31 (Fig. 19) and as a consequence the hydrostatic resistance component from this Froude number onwards is more or less constant and negligible (Orych and Larsson 2015, Eslamdoost *et al.* 2015). Transom stern ventilation decreases the static pressure on the over side of the flap. Further, as the freestream velocity increases, the pressure recovery increases with increase in the flap turning angle. In this regime the balance between the increased hydrostatic resistance due to transom ventilation and
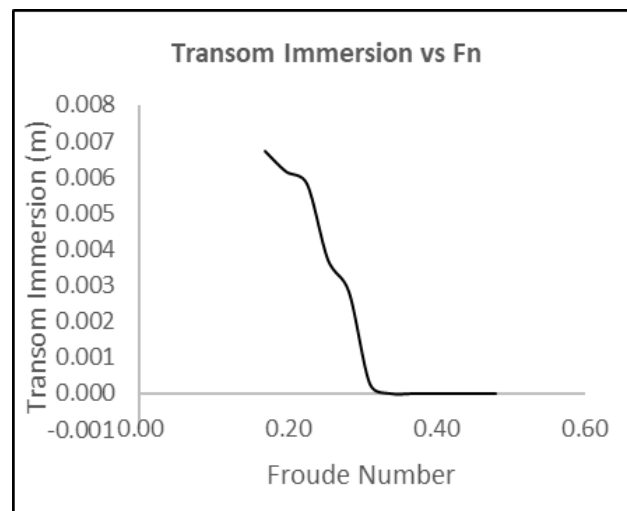
Fig. 19 Transom Immersion vs Froude Number

decreased hydrodynamic resistance by pressure recovery due to induced buttock curvature governs the inception of resistance reduction due to the stern flap as shown in the resistance curves in Fig. 18. For the present hull form, this pressure recovery is only marginal and hence the resistance reduction. In addition to the pressure recovery on the hull, the upward oriented flow suppressed by the stern flap reduces the wave height there by further marginally reducing the resistance.

5.3 High Froude number regime (0.40-0.48)

From the resistance plots at Fig. 18 it is observed that for Froude numbers of 0.40 and above, the advantage of pressure recovery from Stern flap in reducing resistance is more evident with higher flow velocities as compared to low and intermediate Froude numbers. Hydrodynamic resistance decreases rapidly with the increase in the Froude number. At these Froude numbers in addition to pressure recovery by flap which is maximum, the increase in the effective length of the ship by lengthening of transom hollow positively contributes to the decrease in resistance. In this regime although, the 15º flap caused highest pressure under the hull and highest transom hollow lengthening, it did not translate in to resistance reduction because the difference is the pressure experienced by the high pressure flow from underneath the flap caused the stern wave height to substantially increase as it left the flap. However, in the case of 10º flap the pressure increase translated in to a forward component causing resistance reduction and did not lead to an increase in wave height as in 15º flap condition. Further, transom hollow lengthening also occurred. In case of 5º flap, although there was no increase in the wave height, the pressure recovery was not adequate to cause any appreciable decrease in the resistance.

6. Conclusions

Important conclusions of the present study are: -

•   Increase in the flap turning angle decreased the flow velocity along the concave curvature introduced by the Stern flap.
•   Static pressure recovery increased at a point where the flap meets the transom hull as the turning angle increased, thereby increasing the forward component of pressure force.
•   Stern wave height increased as the flap turning angle increased beyond 10° which is the limiting criteria of optimizing flap turning angle for increased transom under side pressure for resistance reduction.
•   In dry transom regime, the length and depth of transom hollow increased with flap turning angle. No appreciable change in the width was observed. Increase in the effective length of the hollow positively contributes to the decrease in the resistance, provided there was adequate pressure increase and reduction in wave heights. Detailed experimental studies on transom flow modification are underway at the time of submission of this paper for publication.

Acknowledgements

References

Cave, C. (1993), "Effect of stern flaps on powering performance of the FFG-7 class", **30**(1), 39-50.
Doctors, L. (2006), "Influence of the transom-hollow length on wave resistance", *Proceedings of the 1st International Workshop on Water Waves and Floating Bodies (21 IWWWFB)*, Loughborough, England.
Doctors, L., Macfarlane, G.J. and Young, R. (2007), "A study of transom-stern ventilation", *Int. Shipbuild. Progress*, **54**(2-3), 145.
Eslamdoost, A., Larsson, L. and Bensow, R. (2015), "On transom clearance", *Ocean Eng.*, **99**, 55-62. doi: 10.1016/j.oceaneng.2015.02.008.
Hemanth Kumar, Y. and Vijayakumar, R. (2018a), "Review of hydrodynamic performance of stern flap", *Proceedings of the International Conference on Computational and Experimental Marine Hydrodynamics MARHY 2018, 26-27 November 2018*, IIT Madras, Chennai, India. Chennai.
Hemanth Kumar, Y. and Vijayakumar, R. (2018b) "Stern flaps : A cost-effective technological option for the Indian shipping industry", *Maritime Affairs: J. National Maritime Foundation of India*, **14**(2), 26-37. Available at: https://doi.org/10.1080/09733159.2018.1562454.
John, S., *et al*. (2011), "Hydrodynamic performance enhancement using stern wedges", Stern Flaps and Interceptors", *Proceedings of the International Conference in Ship & Offshore Technology. Kharagpur*, India.

Karafiath, G., *et al.* (2001), "Hydrodynamic efficiency improvements Ft WPB ISLAND class patrol boats to the USCG 110", **109**, 197-220.

Karafiath, G., Cusanelli, D.S. and Lin, C.W. (1999), "Stern wedges and stern flaps for improved powering–US Navy experience", *T. Soc. Naval Archit. Marine Engineers*, **107**, 67-99.

Lars Larsson, W.S. (2010), The Principles of Naval Architecture Series:Resistance.

Maki, A., *et al.* (2016), "Fundamental research on resistance reduction of surface combatants due to stern flaps", *J. Marine Sci. Technol. (Japan)*, **21**(2), 344-358. doi: 10.1007/s00773-015-0356-8.

Orych, M. and Larsson, L. (2015), "Hydrodynamic aspects of transom stern optimization", 10-12.

Thornhill, E., Cusanelli, D. and Cumming, D. (2008), "Stern flap resistance reduction for displacement hulls", *Proceedings of the 27th Symposium on Naval Hydrodynamics*, 3(October).

Yamano, T., Kusunoki, Y., Kuratani, F., Ogawa, T. and Teturo Ikebuchi, I. F. (2003), "Effect of transom stern bottom profile form on stern wave resistance− A consideration on the effect of real stern end immersion", *J. Kansai Soc.N.A.,Japan*, (**240**), 9.

QM